JOURNAL OF MATERIALS SCIENCE: MATERIALS IN MEDICINE **16** (2005) 429–440

In vivo assessment of hydroxyapatite and silicate-substituted hydroxyapatite granules using an ovine defect model

N. PATEL[1], R. A. BROOKS[2], M. T. CLARKE[2], P. M. T. LEE[2], N. RUSHTON[2], I. R. GIBSON[3], S. M. BEST[1,*], W. BONFIELD[1]
[1]*Department of Materials Science and Metallurgy, University of Cambridge, New Museums Site, Pembroke Street, Cambridge, CB2 3QZ, UK*
E-mail: smb51@cam.ac.uk
[2]*Orthopaedic Research Unit, University of Cambridge, Box 180, Addenbrooke's Hospital, Hills Road, Cambridge, CB2 2QQ, UK*
[3]*School of Medical Sciences, Institute of Medical Sciences, University of Aberdeen, Fosterhill, Aberdeen, AB25 2ZD, UK*

Phase pure hydroxyapatite (HA) and two silicate-substituted hydroxyapatites (0.8 and 1.5 wt% Si, or 2.6 and 4.9 wt% SiO_4) were prepared by aqueous precipitation methods. The filter-cakes of HA and silicate-substituted hydroxyapatite (SiHA) compositions were processed into granules 1.0–2.0 mm in diameter and sintered at 1200 °C for 2 h. The sintered granules underwent full structural characterisation, prior to assessment in an ovine defect model by implantation for a period of 6 and 12 weeks. The results indicate that HA and SiHA implants were well accepted by the host tissue, with no evidence of inflammation. New bone formation was observed directly on the surfaces and in the spaces between the granular implants. Quantitative histomorphometry as determined by the percentage of bone ingrowth and bone coverage for both SiHA implant compositions was significantly greater than that for phase pure HA. These findings indicate that the *in vivo* bioactivity of hydroxyapatite was significantly improved by the incorporation of silicate ions into the HA structure, making SiHA ceramics attractive alternatives to conventional HA materials for use as bone graft substitute ceramics.
© *2005 Springer Science + Business Media, Inc.*

1. Introduction

Currently, autografts and allografts are the preferred choice of bone grafting materials, with synthetic materials representing only a small percentage of the total number of procedures [1, 2]. Although, hydroxyapatite [$Ca_{10}(PO_4)_6(OH)_2$; HA] has achieved significant interest as a synthetic bone graft material [3–6] its clinical use has been limited. HA is osseoconductive *in vivo* [7], which is due largely to the chemical similarity of HA and bone mineral. A disadvantage in using HA implants in comparison to some bioactive glasses and glass-ceramics is that the rate at which bone apposes and integrates with HA is relatively slow [8, 9]. Consideration of the complex chemistry of bone mineral may provide an explanation for the slow rate of osseointegration of HA implants. Although bone mineral is essentially a calcium phosphate, it also contains significant concentrations of other ions that can substitute for the different cation and anions present in the apatitic structure. The type and amount of ionic substitution in the apatite phase varies from the wt% level (e.g. CO_3^{2-}) to the ppm—ppb level (e.g. Mg^{2+} or Sr^{2+}). These ionic substitutions induce complex structures at the unit-cell level and play a role in influencing the dissolution rate and bioactivity of bone mineral [10–12].

The role of silicon in bone has been investigated since the early 1970s. Carlisle [13–15] reported that silicon (≈5 wt%) was observed in active growth areas, such as the osteoid of the young bone of mice and rats and that silicon deficiency resulted in abnormal skeletal development. Similar studies by Schwarz and Milne [16] reported that silicon deficiency in a rat model led to skull deformations, resulting in nodular poorly defined mineral crystals, indicative of a primitive type of bone. Studies have also demonstrated a relationship between the level of dietary silicon and bone mineralisation. An increase in silicon intake was correlated by accelerated bone mineralisation [17]. Furthermore, recent *in vitro* studies have shown that physiological levels of silicon (10–20 μM) in the form of orthosilicic acid stimulated

*Author to whom all correspondence should be addressed.

type I collagen synthesis in human osteoblast-like cells and also enhanced osteoblastic cell differentiation [18].

Since physiological levels of silicon have a beneficial role in bone calcification and metabolism, it may be hypothesised that the incorporation of comparable levels of silicate ions into the structure of HA may also enhance the bioactivity of these implants. Although, several attempts have been made to prepare silicate-substituted hydroxyapatites by a variety of synthesis methods, the majority of these studies have resulted in silicon-containing apatites with undesirable secondary phases and/or additional ionic substitutions [19–23]. For example, Leshkivich and Monroe [22] and Boyer *et al.* [23] prepared co-substituted silicon-containing hydroxyapatites by solid-state methods, these materials, however, required the substitution of a second ion, such as lanthanum or sulphate, in addition to silicate. Furthermore, neither of these studies resulted in a phase-pure silicate-substituted hydroxyapatite (SiHA). Recent studies by Gibson *et al.* [24–26] have described the preparation of a range of SiHAs by aqueous precipitation methods involving calcium hydroxide, orthophosphoric acid and silicon tetra-acetate solutions. X-ray diffraction studies indicated that the samples prepared in this manner were phase pure with no extraneous secondary phases. In addition, samples with up to 1.6 wt% of silicon substitution were reported [24–26].

To date, the number of studies reporting the biological response to SiHAs is limited. *In vitro* studies by Gibson *et al.* [27] demonstrated that osteoblast-like cell activity was significantly enhanced on SiHA ceramics compared to HA. In addition, the time taken to induce the formation of a poorly crystalline surface apatite layer on 0.8 wt% SiHA ($\approx$7 days) was significantly faster than HA (24–28 days) samples, incubated in simulated body fluid (SBF) [27]. Recent *in vivo* studies by Patel *et al.* [28] demonstrated that the percentage of bone ingrowth for 0.8 wt% SiHA (37.5% $\pm$ 5.9) was significantly greater than that for HA granules (22.0% $\pm$ 6.5) when implanted into the femoral condyle of a rabbit model for 23 days. In addition, both, mineral apposition rate and the percentage of bone/implant coverage for 0.8 wt% SiHA were reported to be significantly greater than HA implants [28]. Nevertheless the mechanisms by which silicate ions increase the *in vitro* and *in vivo* bioactivity of HA is still unresolved. In addition, the longer-term biological response to SiHA implants has not been evaluated.

The aim of this present study was to quantitatively compare the longer-term *in vivo* response of SiHA and HA granules using an ovine femoral condyle defect model. It was hypothesised that the results obtained from this study in conjunction with the *in vivo* results reported in the previous rabbit femoral condyle model study [28] will provide for an improved understanding of the mechanism(s) underlying the inherent bioactivity of SiHA ceramics.

2. Materials and methods

2.1. Sample preparation

Synthetic HA was prepared by the conventional aqueous precipitation reaction between calcium hydroxide, $Ca(OH)_2$, and orthophosphoric acid, H_3PO_4, solution according to the methods described elsewhere [29–31]. The concentrations of reactants were made up according to the required Ca/P molar ratio of 1.667, corresponding to phase pure stoichiometric HA.

SiHA samples were prepared in a similar manner to HA according to the methods described by Gibson *et al*. [24]. Here, in addition to calcium hydroxide and orthophosphoric acid solution, silicon tetra-acetate [SiAc; $Si(CH_3CO_2)_4$] was incorporated into the reaction mixture as the source of silicate ions. The quantities of reactants were calculated to produce 0.8 and 1.5 wt% silicon or 2.6 and 4.9 wt% silicate-substituted hydroxyapatite, by assuming that silicate ions would substitute for the phosphate sites in the HA lattice.

The process used to prepare green granules of HA, 0.8 wt% SiHA (0.8SiHA) and 1.5 wt% SiHA (1.5SiHA) involved two steps. First, the dried filter-cakes were partially ground using a porcelain pestle and mortar. Second, the partially ground filter-cakes were mechanically sieved for 1 h at an amplitude of 1.00 mm using a Retsch AS 200 mechanical sieve shaker and ISO standard stainless steel sieves. This process produced green granules, 1–2 mm in diameter. The green granules of HA and SiHA samples were subsequently sintered in a Lenton UAF 14/10 chamber furnace at a temperature of 1200 °C using a ramp rate of 2.5 °C per minute, dwell time of 2 h and a cooling rate of 10 °C per minute to ambient temperature.

The sintered granules were assessed for their phase purity, chemical content and Ca/P molar ratio by X-ray diffraction (XRD), CHN analysis and X-ray fluorescence (XRF) spectroscopy, respectively. The absolute density and packing density of the granules was determined using a Micromeritics Accupyc 1330 Pycnometer and a Micromeritics Geopyc 1360 Envelope Density Analyser, respectively. The sintered granule size was determined using a Malvern Mastersizer 2000 particle size analyser.

The micro- and macrostructure of the sintered granules were studied by scanning electron microscopy). Grain size studies were made on polished (1 μm finish) and etched (10 vol% H_3PO_4) samples.

2.2. Implantation procedure

The UK Home Office code of practice was adhered to at all times for the performance of all regulated procedures under the authority of appropriate project and personal licences issued in accordance with the Animals (Scientific Procedures) Act 1986 to include all husbandry and welfare considerations.

All implantations were performed on 2–3 year old Texcel $\times$ Continental sheep weighing between 70–80 kg. Implants were placed bilaterally into the femoral condyle of the hind legs of the sheep. This site was selected as it presented a large volume of load-bearing cancellous bone. All implant compositions were implanted for two time periods: 6 and 12 weeks. For each implant composition and time point, 4 implants were performed. Fig. 1 shows a schematic diagram of the position of the implant.

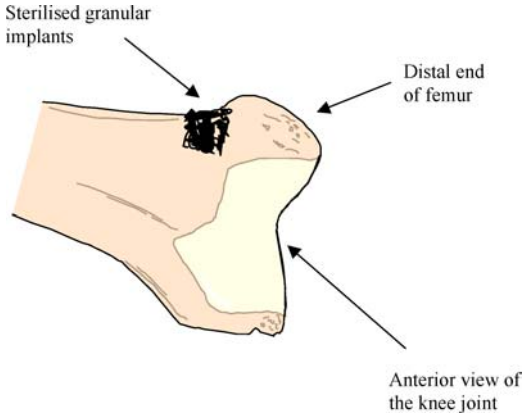

Figure 1 A schematic diagram of the position of the implant.

Implantations were randomised in such a way that the composition of the right leg implant was different to that in the left leg for each animal. Food was withdrawn for 24 h prior to surgery. Xylazine (0.2 mg kg^{-1}) was administered as a premedication sedative. Augmentin (1 g/sheep) and Flunixin Meglumine (1.1 mg kg^{-1}) were given to provide antibiotic and analgesic cover, respectively. The animals were anaesthetised with diazepam (0.15 mg kg^{-1}) and ketamine (2.5 mg kg^{-1}) and maintained with halothane. The right hind limb was clipped, scrubbed and draped for sterile surgery. An incision was made adjacent to the femoral condyle and the soft tissue was dissected to reveal the underlying bone. A defect, 9 mm in diameter and 9 mm in depth, was created within the bone using custom-made drill bits (R.J. Layland (Surgical) Engineering) and a pneumatic air drill. The defect site was subsequently irrigated with sterile saline solution and the granules were poured into the defect using a custom-made implant applicator device that ensured all the granules occupied the defect site. After implantation, the incisions were closed using interrupted suturing. The process was repeated on the left hind leg, with granules of a different composition and anaesthesia was reversed with atipamazole. Three separate fluorochrome labels were administered at 14 days (calcein green, 15 mg kg^{-1}), 8 days (alizarin red, 40 mg kg^{-1}) and 3 days (tetracycline, 40 mg kg^{-1}) before sacrifice by intravenous injection via the cephalic vein.

Sheep were killed at 6 and 12 weeks after surgery by an intravenous overdose of barbiturates and the distal femora were dissected. Radiographs of the femur were obtained perpendicular to the direction in which the implants were placed.

2.3. Histological evaluation

The trimmed femurs containing the implants were fixed in 4% w/v of paraformaldehyde solution for 24 h. After fixation, the samples were washed in phosphate buffered saline solution for 3 h and subsequently dehydrated and de-fatted under vacuum pressure (600 mBar) using increasing concentrations of alcohol followed by acetone. The femurs were subsequently infiltrated and embedded in polymethyl methacrylate (PMMA) resin. Sectioning of the undecalcified resin blocks was performed parallel to the longitudinal axis of the femur using a Struers Accutom 5 cutting machine. The cut sections were bonded to Plexiglass slides (Medenex, Bath, UK) using epoxy resin and subsequently ground and polished to a thickness of 50–75 μm. A total of three sections were cut, ground and polished per implant. Two sections were stained at 60 °C for 1 h with 0.9% w/v toluidine blue solution for histology and histomorphometry and one section per implant was left unstained for fluorochrome evaluation. Stained sections were studied for histology by transmitted light illumination using a Leica DMRXA2 optical microscope and the unstained sections were studied under a Leica DMRXA2 reflected light fluorescence microscope to detect the fluorochrome labels.

2.4. Histomorphometry

The percentage of bone ingrowth and bone coverage within an implant was determined using Weibel [33] and Merz grids [34], respectively. A series of micrographs were taken for each section. These micrographs were stitched together to form a collage of the whole section. Each collage was then split into nine zones. Histomorphometry was performed on each of the zones to build a map of bone ingrowth and coverage within each section. Detailed descriptions of the methods used for histomorphometry can be found elsewhere [28, 35].

Statistical analysis was carried out using analysis of variance with differences between individual treatments compared by post-hoc testing with Bonferroni correction. Significance was set at the 5% level. Testing was carried out using SPSS Version 10 software (SPSS, Inc., Chicago, USA).

3. Results

3.1. Chemical analysis

As indicated in Fig. 2, analysis of the samples by XRD illustrated that for a sintering temperature of 1200 °C the products were phase pure and contained no secondary phases, such as tricalcium phosphate (TCP) or

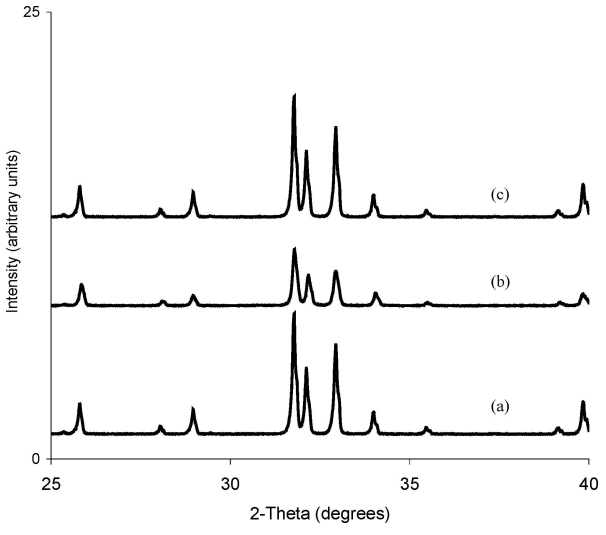

Figure 2 XRD traces for sintered: (a) HA, (b) 0.8SiHA, and (c) SiHA granules.

TABLE I Expected and measured silicon content and molar ratios for HA, 0.8SiHA and 1.5SiHA samples

Sample	Ca/P ratio (expected)	Ca/(P + Si) ratio (expected)	wt% Si (expected)	Ca/P ratio (measured)	Ca/(P + Si) ratio (measured)	wt% Si (measured)
HA	1.67	1.67	0	1.67	1.67	0.03
0.8SiHA	1.75	1.67	0.8	1.76	1.67	0.84
1.5SiHA	1.83	1.67	1.5	1.84	1.66	1.53

TABLE II Carbon contents of as-prepared and sintered samples, determined by C-H-N analysis

Sample	Carbonate content of as-prepared samples (wt%)	Carbonate content of sintered samples (wt%)
HA	1.01	<0.10
0.8SiHA	4.42	<0.10
1.5SiHA	9.17	<0.10

calcium oxide (CaO). In addition, as highlighted in Table I, the expected Ca/P molar ratios for HA and SiHA samples were in good agreement with the values measured by XRF. For the stoichiometric HA sample, the Ca/P and Ca/(P + Si) molar ratios were equivalent (≈ 1.67), as would be expected for silicon-free samples. The measured amounts of silicon (wt%) are also included in Table I. Only trace levels of silicon were detected in the stoichiometric HA sample, whereas the amounts of silicon measured in the 0.8SiHA (0.84 wt%) and 1.5SiHA (1.53 wt%) samples were very close to the design values of 0.8 and 1.5 wt%, respectively.

The carbonate contents (wt%) of as-prepared and sintered samples are listed in Table II. The as-prepared stoichiometric HA sample contained 1.01 wt% carbonate, which was a result of precipitation at high pH and was associated with adsorbed carbonate rather than structural carbonate groups; this was demonstrated by the complete loss of these groups on sintering. In contrast, the carbon content increased with silicon content for the as-prepared SiHA samples. The high levels of carbon detected in as-prepared SiHA samples may be due to the combination of the presence of carbon in the silicon tetra-acetate precursor and as a result of precipitation at high pH.

3.2. Physical characterisation

The bulk densities of as-prepared and sintered granules of HA and SiHA samples are represented in Table III. The green densities of all compositions were between 52–59% of the theoretical value for HA (3.156 g cm^{-3}). The sintering process resulted in an increase in density (96–99%) for all sample compositions. The packing

TABLE III Density results for HA, 0.8SiHA and 1.5SiHA granules

Sample	Green density density(g cm^{-3})	Sintered density (g cm^{-3})	Sintered packing density (g cm^{-3})
HA	1.643 [0.006]	3.047 [0.007]	1.255 [0.012]
0.8SiHA	1.821 [0.003]	3.145 [0.015]	1.376 [0.008]
1.5SiHA	1.854 [0.021]	3.141 [0.004]	1.383 [0.006]

[Standard deviations in square parentheses].

TABLE IV Sintered granule size for HA and SiHA compositions, measured by laser diffraction

	Granule Size (μm)		
Sample	$d(0.1)$	$d(0.5)$	$d(0.9)$
HA	706.85	1102.00	1609.82
0.8SiHA	664.67	1008.87	1493.71
1.5SiHA	597.15	1000.29	1535.38

$d(0.5)$ is the size in microns at which 50% of the sample is smaller and 50% is larger.
$d(0.1)$ is the size of granule below which 10% of the sample lies.
$d(0.9)$ is the size of granule below which 90% of the sample lies.

TABLE V Mean and modal grain sizes of sintered HA, 0.8SiHA and 1.5SiHA microstructures ($n \geq 100$)

Sample	Mean grain size (μm)	Mean grain size (μm)
HA	1.11 [0.53]	0.99
0.8SiHA	0.69 [0.28]	0.47
1.5SiHA	0.45 [0.17]	0.37

[Numbers in square parenthesis are standard deviations].

(TAP) densities of sintered HA and SiHA samples are also listed in Table III. The packing density for all samples were similar (39–44% of the theoretical value for HA) indicating that approximately the same mass of granules will be required to fill a defect of known volume, irrespective of sample composition. The sintered granule size for HA and SiHA compositions are listed in Table IV. The median granule size ranged from approximately 1000–1100 μm in diameter. Silicate substitution did not appear to affect the particle size of the sintered granules.

The SEM images presented in Fig. 3 highlight that silicate substitution did not affect the morphology of the sintered granules. Both, HA and SiHA granules were angular in morphology. The effect of silicate substitution on the sintered microstructure of the HA granules was clearly evident in Fig. 4. Image analysis results presented in Table V show a decrease in grain size with an increase in silicon content. The grain sizes measured in this study ranged from sub-micron levels for SiHA samples to approximately 1 μm for the non-substituted HA sample.

3.3. Histological evaluation

Post-mortem examination revealed no abnormalities over the site of the operation. Normal healing of the soft tissues had occurred. After retrieval of the femora, the granular ceramics were not visible due to the presence of the periosteum. This was observed for both 6- and

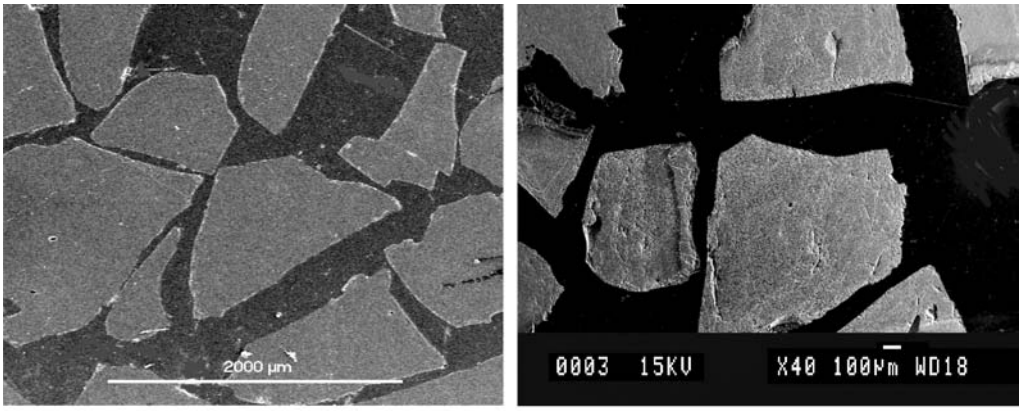

(a) (b)

Figure 3 SEM images of sintered: (a) HA and (b) 0.8SiHA granules.

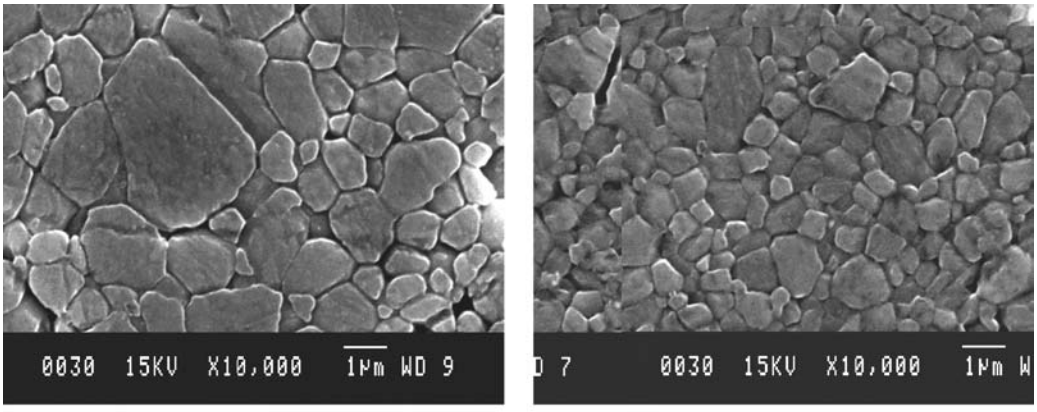

(a) (b)

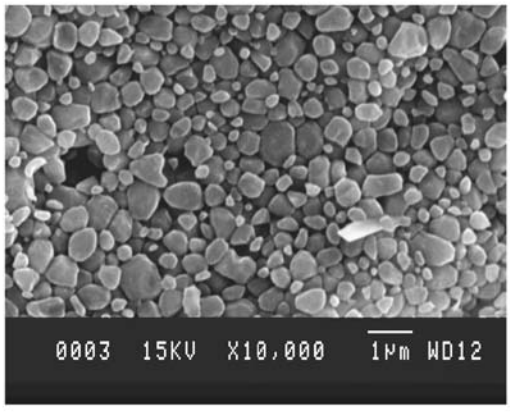

(c)

Figure 4 Sintered microstructures of (a) HA, (b) 0.8SiHA, and (c) 1.5SiHA granules.

12-week implants. In most cases the defect site was indistinguishable from the surrounding un-operated bone and radiographs were required to locate the implants; Fig. 5 shows a typical radiograph of the sheep femoral condyle, showing the location of the granular implant.

Histological evaluation indicated that new bone had formed in the spaces between granules for all implant compositions and time-points. There was evidence of direct bone apposition on the surface of all implants, with no evidence of fibrous encapsulation. Favourable cells such as osteoblasts and osteocytes were observed in close proximity to the surface of the granular implants, with active areas of bone deposition, resorption and remodelling occurring within both 6- and 12-week implants. For all implant compositions, bone ingrowth proceeded from the deep end and from the walls of the defect. Complete bone integration was not observed for any implant composition at the two different time points.

At 6 weeks *in vivo*, new bone appeared to adhere to the surface of the HA granules from the distal (deep) end of the defect. Bone bridging had occurred between some of the HA granules within this region (Fig. 6(a)). Osteocytes were present in close proximity to the granule surfaces. In many regions, the osteocytes were not arranged in an orderly manner, which was indicative of

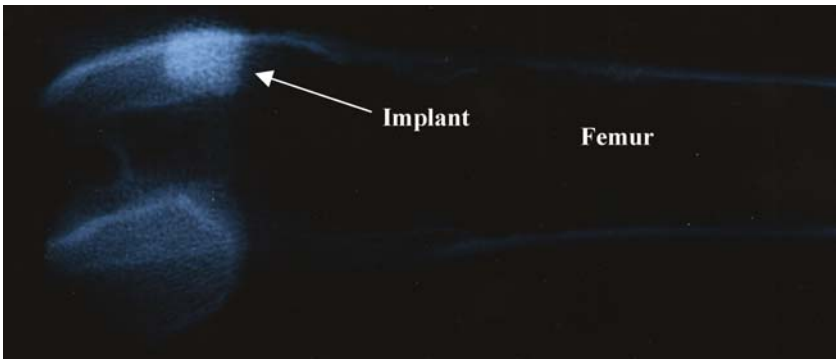

Figure 5 Radiograph of a sheep femoral condyle showing the position of the granular implant.

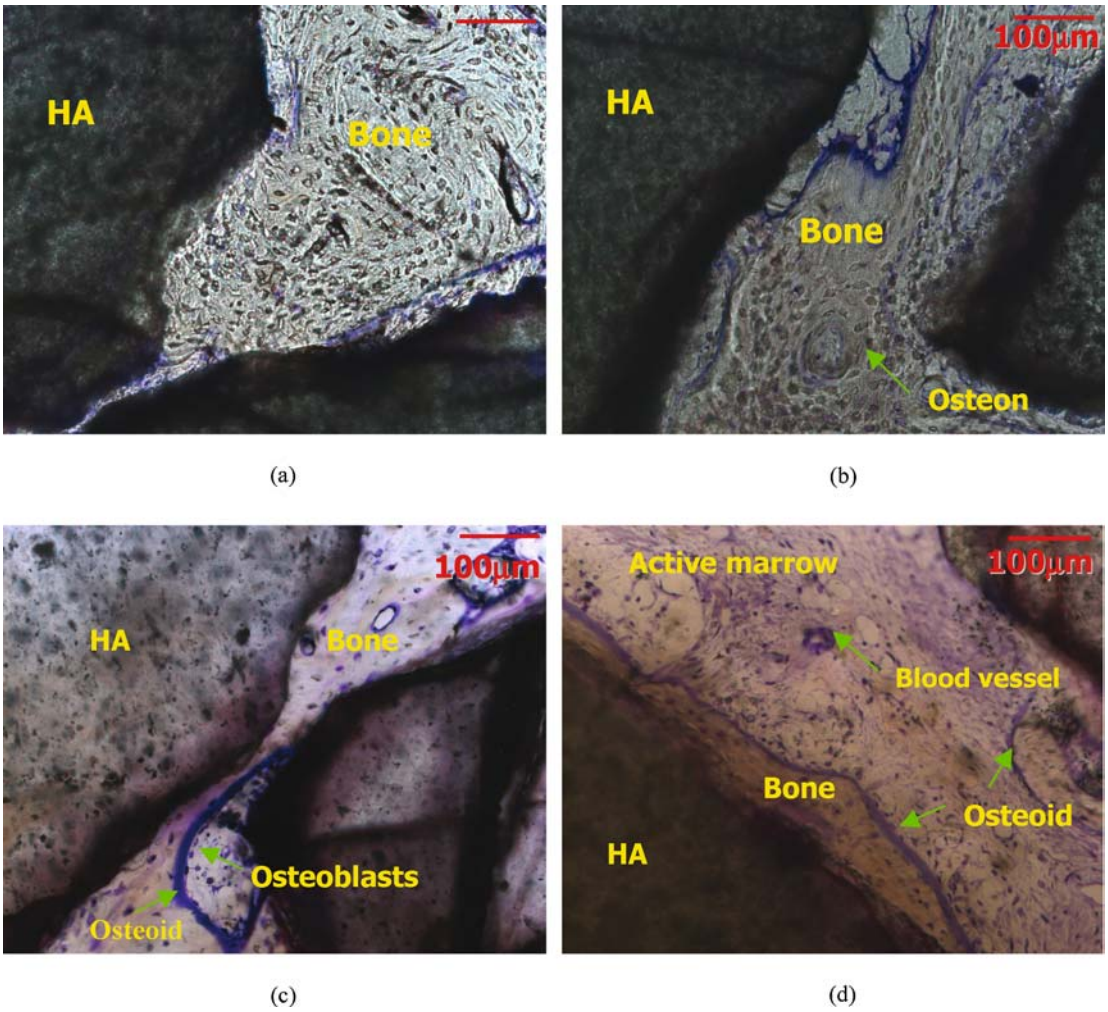

Figure 6 Histological appearance of HA implants at 6 weeks showing: (a) bone bridging between granules, (b) the presence of an osteon, (c) heavily stained osteoid lined by osteoblasts and (d) active marrow in close proximity to the granule surfaces.

woven bone that had formed rapidly. Furthermore, as highlighted in Fig. 6(b) and (c), osteons and osteoblasts were observed in some regions of newly formed bone in close proximity to the HA implants. Very little, if any, new bone was observed in the medial and superior regions of the HA implants at 6 weeks *in vivo*. As indicated in Fig. 6(d), these regions were characterised by a cellular mesh of active marrow associated with normal wound healing. Some of the cells within this region were clearly active, with the presence of osteoid and osteoblasts. In addition, the active marrow contained blood vessels and appeared to be recruiting osteoblasts to form bone.

The amount of new bone formation within HA implants increased from 6 to 12 weeks. As indicated in Fig. 7, direct bone apposition was observed on the surface of HA granules and large areas of new bone had formed within the spaces between HA granules at 12 weeks (Fig. 7(b)). In some regions, highlighted in Fig. 7(c), osteoid, lined by seams of osteoblasts, were observed depositing bone within HA implants. Furthermore, Fig. 7(d) indicates that some areas of new bone were characterised by remodelling units. Some of the active marrow observed for the 6-week HA implants was replaced by new bone in the 12-week implants.

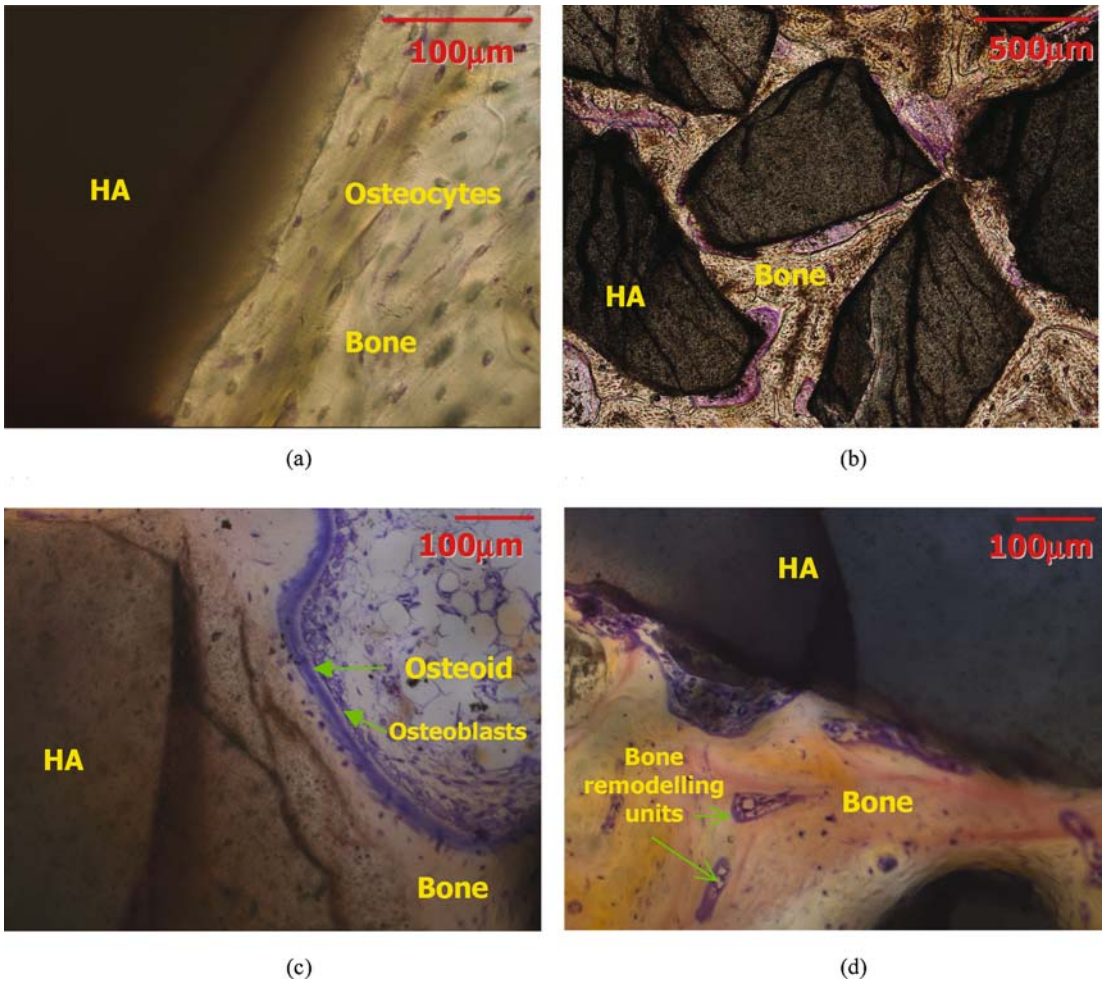

Figure 7 Histology images showing: (a) direct bone apposition, (b) bone bridging between granules, (c) the presence of heavily stained osteoid and osteoblasts and (d) remodelling units within HA implants at 12 weeks *in vivo*.

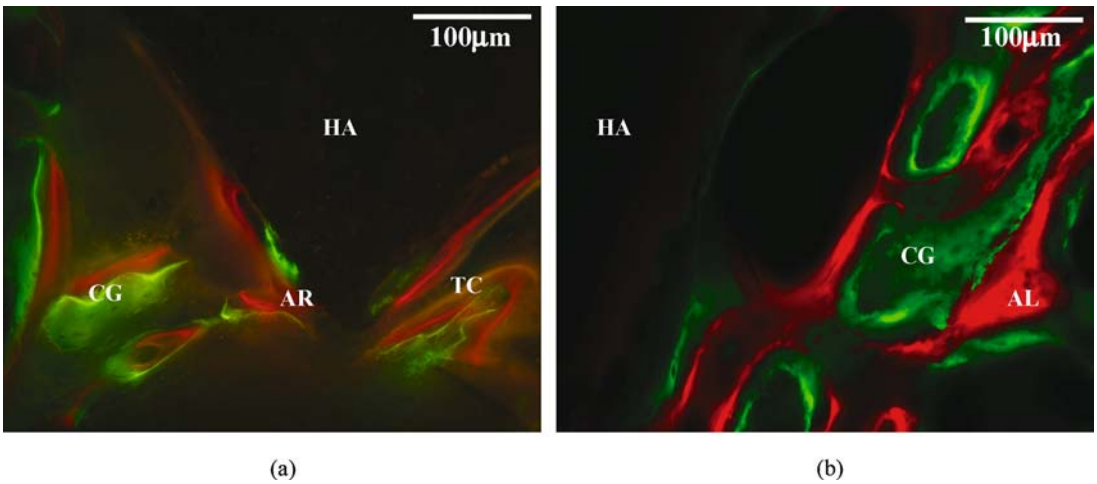

Figure 8 Fluorochrome labelled bone demonstrating bone deposited in the distal (deep) regions of HA implants after: (a) 6 weeks and (b) 12 weeks *in vivo*. [Calcein green = CG; Alizarin red = AR and Tetracycline = TC].

The optical fluorescence microscopy results, presented in Fig. 8, indicate the presence of calcein green, alizarin red and tetracycline fluorochrome bone marking labels in the bone tissue surrounding the HA implants within the distal (deep) end of HA implants, after 6 and 12 weeks *in vivo*.

The histological appearance of 0.8SiHA and 1.5SiHA implants was similar to HA. Large areas of bone ingrowth were observed in the distal (deep) regions of 0.8SiHA implants at 6 weeks, with extensive bone bridging occurring between the granular surfaces. In some regions osteoid appeared in close proximity to the granules (see Fig. 9(a)). The medial and superior regions of 0.8SiHA implants were infiltrated by active marrow at 6 weeks. A greater degree of bone regeneration and bone bridging between granules was observed for 0.8SiHA implants at 12 weeks. Fig. 9(b) and (c) shows the histological response to 0.8SiHA implants

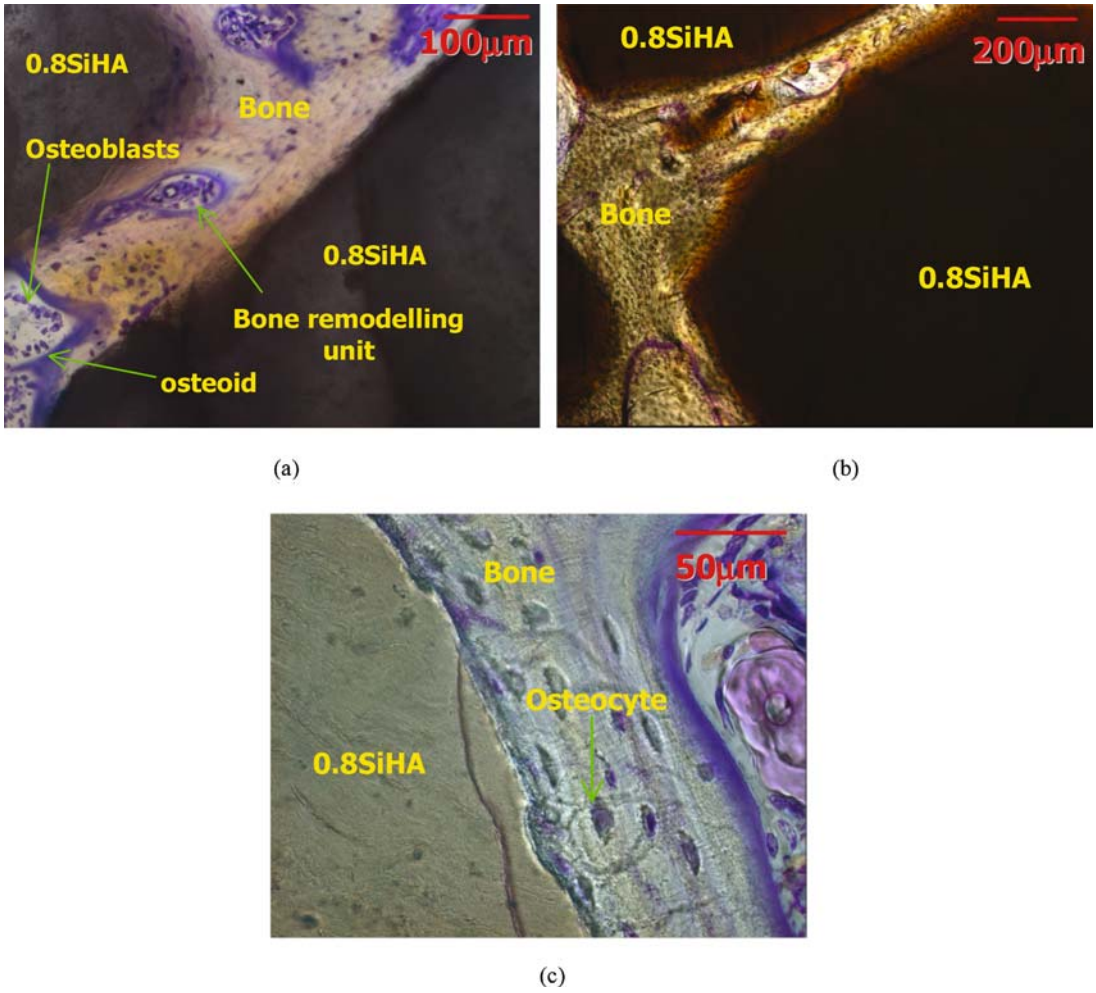

Figure 9 Histological appearance of 0.8SiHA implants at: (a) 6 weeks *in vivo* (b) 12 weeks *in vivo* showing bone bridging between granules and (c) a high magnification image showing direct bone apposition to 0.8SiHA at 12 weeks *in vivo*.

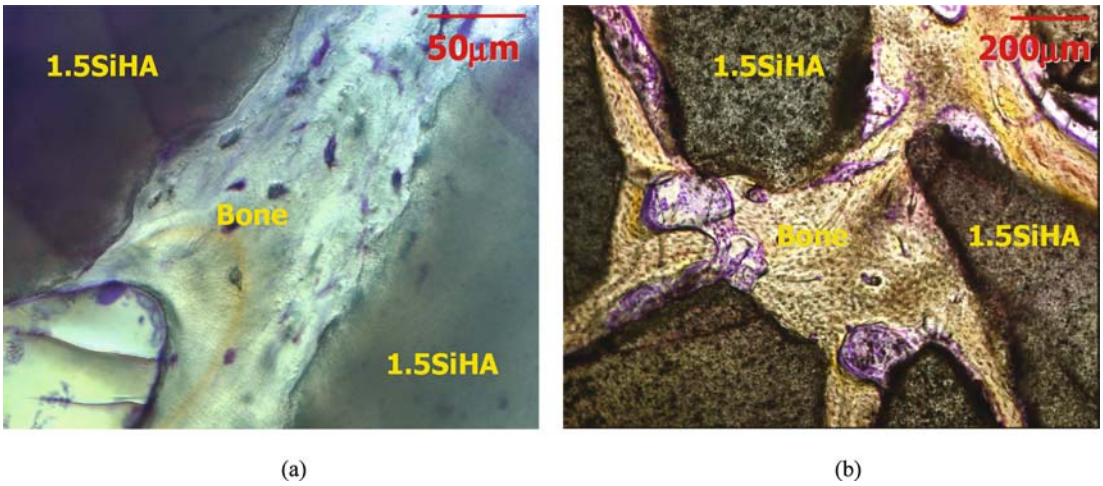

Figure 10 Histological appearance of 1.5SiHA implants at: (a) 6 weeks and (b) 12 weeks *in vivo*.

at 12 weeks. The histological appearance of 1.5SiHA implants was similar to 0.8SiHA implants at 6 and 12 weeks *in vivo*. As highlighted in Fig. 10, large areas of new bone, characterised by regions of active bone formation, were observed in the spaces between 1.5SiHA granules. The optical fluorescence microscopy results for 0.8SiHA and 1.5SiHA implants were comparable to HA. Fig. 11 highlights the presence of calcein green, alizarin red and tetracycline labelled bone within 0.8SiHA and 1.5SiHA implants at 6 and 12 weeks.

3.4. Histomorphometry

Quantitative and statistical assessment of the absolute area of bone ingrowth within the implants confirmed that the percentage of bone ingrowth increased with implantation time. Fig. 12 shows the absolute percentage of bone ingrowth for 0.8SiHA and 1.5SiHA implants was significantly greater than HA implants at both, 6 and 12 weeks.

The area of bone coverage for HA, 0.8SiHA and 1.5SiHA implants are presented in Fig. 13. A significant

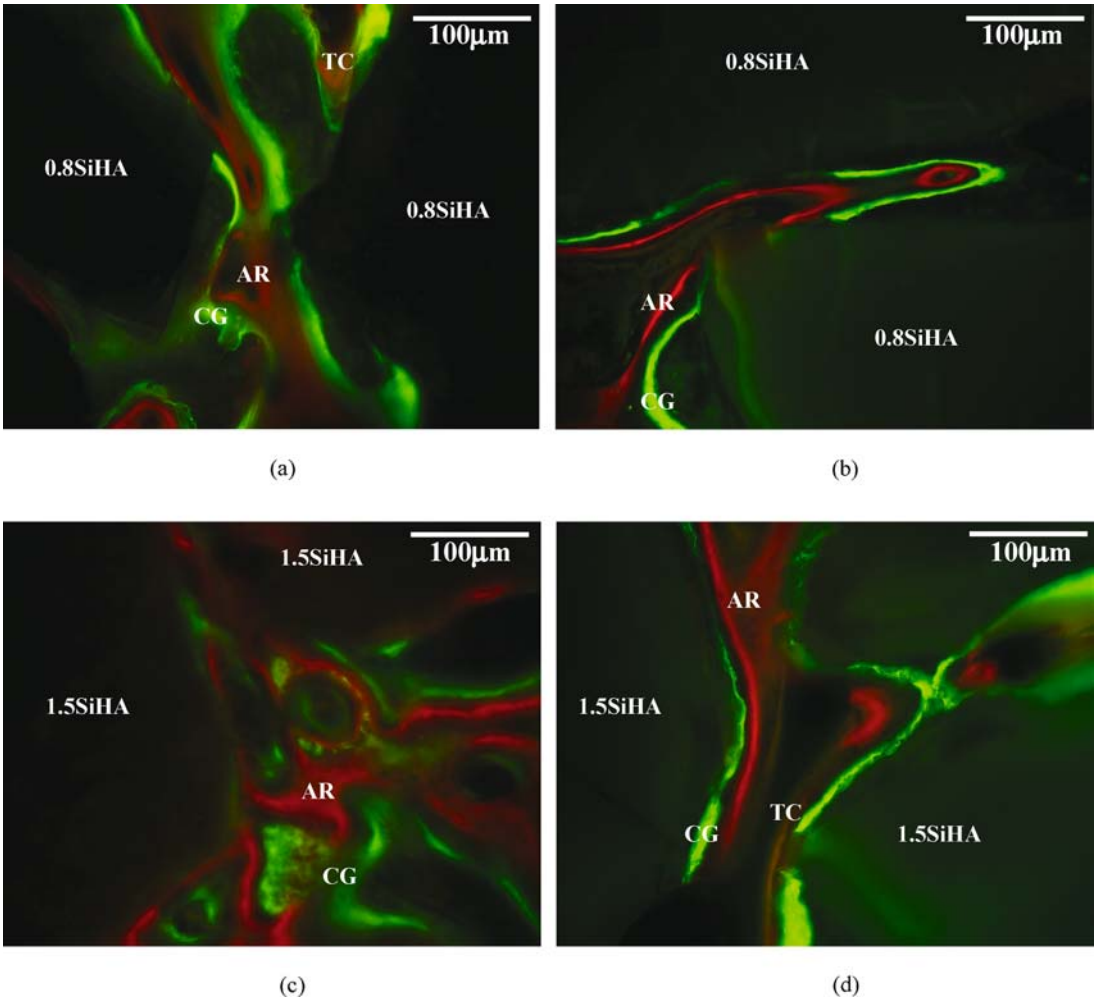

Figure 11 Fluorochrome labelled bone within: (a) 0.8SiHA at 6 weeks, (b) 0.8SiHA at 12 weeks, (c) 1.5SiHA at 6 weeks and (d) 1.5SiHA at 12 weeks *in vivo*. [CG = calcein green, AR = alizarin red and TC = tetracycline].

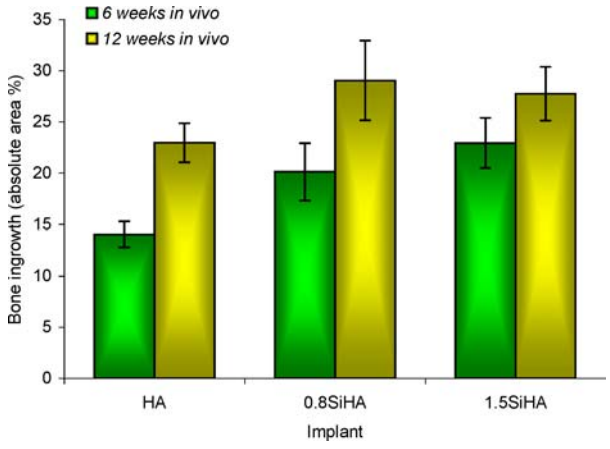

Figure 12 Absolute percentage of bone ingrowth in HA, 0.8SiHA and 1.5SiHA implants at 6 and 12 weeks *in vivo*.

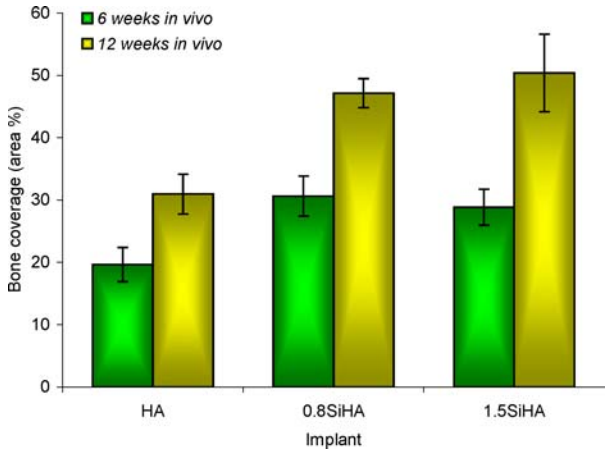

Figure 13 Percentage of bone coverage within HA, 0.8SiHA and 1.5SiHA implants at 6 and 12 weeks *in vivo*.

increase in the percentage of bone coverage was observed from 6 to 12 weeks *in vivo* for implant compositions. Furthermore, the percentage of bone coverage for 0.8SiHA and 1.5SiHA implants was significantly greater compared to HA implants at 6 and 12 weeks.

These findings suggest that the substitution of silicate ions significantly enhanced the bioactivity of HA implants. However, no significant differences in bone ingrowth and coverage were observed between 0.8SiHA and 1.5SiHA implants, suggesting that an increase in silicon substitution (from 0.8 to 1.5 wt%) did not significantly enhance the *in vivo* bioactivity of HA.

4. Discussion

The synthesis route used to prepare HA and SiHA granules was successful, highlighted by chemical purity and stoichiometry, resulting in a single-phase

hydroxyapatite upon sintering. The only significant difference in the chemical composition of sintered HA and SiHA was that of silicon content. A detailed discussion on the chemical synthesis and preparation of dense HA and SiHA granules can be found elsewhere [24, 26, 28].

A cancellous defect ovine model was used to assess the bioactivity of HA and SiHA granules. This model was selected due to the following reasons: (1) the bone metabolism of sheep is more comparable to humans than rodent models [50]; (2) sheep tend to use their treated limbs to support their weight immediately after surgery [51, 52] and (3) the relatively large size of the animal allowed the creation of a larger defect site compared to a smaller animal such as the rabbit. This defect size was capable of accommodating implants approximately 7 times larger (in volume) compared to the defect site previously used in the rabbit model [28]. This site was selected as it ensured that the mechanical stimulation around the implant would encourage bone ingrowth and remodelling. In addition, Flautre *et al.* [53] reported the successful use of similar sheep model to assess the bioactivity of calcium phosphate cements. The authors reported that an unfilled defect showed limited bone regeneration (11%) at 24 weeks *in vivo* [53].

The results from this study indicate that the implantation of HA, 0.8SiHA and 1.5SiHA granules did not produce adverse biological responses. Bone regeneration was observed within all implant compositions. The tissue interface with the implant exhibited regions in which bone was in direct contact with the implant surface. The histological appearance of the regenerated bone and the interface was comparable to that previously observed in a rabbit model [28] and fibrous encapsulation was not observed. In contrast, Flautre *et al.* [53] observed differences in the histological appearance of calcium phosphate cements implanted in sheep and rabbit models. They reported the formation of a fibrous capsule around calcium phosphate cements implanted into the femoral condyle of sheep for a period of 24 weeks. But, fibrous encapsulation was not observed when the same material was implanted into a rabbit model.

In this study bone ingrowth within all implant compositions advanced from the distal (deep) end and from the walls of the defect, i.e., from the most abundant source of potentially osteogenic cells. The medial and superior regions of all implant compositions were infiltrated with active marrow. This tissue was highly cellular and in some regions characterised by the presence of osteoid, osteoblasts and blood vessels. At 12 weeks, the degree of bone ingrowth had increased for all implant compositions. Some of the active marrow observed at 6 weeks had been replaced by bone. These findings suggest that the active marrow contained and/or was recruiting cells for bone formation.

The bioactivity of HA was significantly enhanced by the substitution of 0.8 and 1.5 wt% silicon into the hydroxyapatite structure. This was demonstrated by an increase in the percentage of bone ingrowth and coverage for 0.8SiHA and 1.5SiHA implants compared to HA at 6 and 12 weeks.

Many of the proposed mechanisms underlying the bioactivity of calcium phosphate ceramics have reported that the "bone bonding" ability of these ceramics occurs by the partial dissolution of the ceramic, resulting in elevated concentrations of calcium (Ca^{2+}) and phosphate (PO_4^{3-}) ions within the local environment. Subsequently, the released Ca^{2+} and PO_4^{3-} ions, together with carbonate (CO_3^{2-}) ions and proteins from the biological milieu precipitate resulting in an intermediate carbonate-containing apatite-like layer that forms on the surface of the implant *in vivo* [10, 54–57]. It has been suggested that osteoblasts can preferentially proliferate and differentiate on this apatite-like layer [58, 59]. Since the formation of an apatite-like layer is related to the surface reactivity of the implant, it seems reasonable to assume that the dissolution rates of calcium phosphate implants will influence the rate of formation of an apatite-like surface layer and in turn, influence bone formation on these surfaces. Studies have reported that the physiological degradation processes of calcium phosphates are primarily influenced by the chemical composition, crystallinity, density, surface area and microstructure of the material [10, 54, 60–64]. For example, Daculsi *et al.* [10] reported that the dissolution of calcium and phosphate ions from hydroxyapatite ceramics was initiated at microstructural defects such as dislocations and grain boundaries. Analysis of the microstructures of the granules prepared in this study indicated that the grain boundary surface area for 0.8SiHA and 1.5SiHA granules was greater compared to HA. An increased presence of structural defects, such as grain boundaries, may increase the physiological degradation rates of SiHA compared to HA and may also provide an explanation for the improved bioactivity of SiHA implants compared to HA. In addition, recent research within our laboratory has focussed on high resolution transmission electron microscopy (HR-TEM) studies of 0.8SiHA and 1.5SiHA implants [65, 66]. A greater depth of dissolution was observed at the surface of 0.8SiHA and 1.5SiHA grains compared to HA implants at 6 and 12 weeks *in vivo*. This was demonstrated by larger needle-like apatite crystallites emanating from the deeper regions of 0.8SiHA and 1.5SiHA implants compared to the smaller plate-like apatite crystallites at the HA-bone interface. In addition, a greater number of triple-junctions and sub-grain boundaries were observed in 0.8SiHA and 1.5SiHA compared to HA and their dissolution was initiated at these defect sites *in vivo* [66].

Further HR-TEM studies have examined the bone/implant interface of HA, 0.8SiHA and 1.5SiHA implants. A notable finding was the difference in apatite deposits at the surface of HA, 0.8SiHA and 1.5SiHA implants. Organised collagen fibrils were observed at the 0.8SiHA and 1.5SiHA-bone interface after 6 weeks. In contrast, organised collagen fibrils were only observed after 12 weeks around HA implants [65]. These findings suggest that the bone apposing the 0.8SiHA and 1.5SiHA implants was at a more developed stage, and corroborate *in vitro* findings of enhanced osteoblast-like cell attachment on SiHA ceramics [27]. Although, the results reported by Porter

et al. [65, 66] suggest that a solution-mediated process enhances the bioactivity of 0.8SiHA and 1.5SiHA implants, it is important to consider the effects of silicate ions. The preferential dissolution of silicate ions from 0.8SiHA and 1.5SiHA implants may also play a role in accelerating the process of bone formation and mineralisation around the implant. Studies have elaborated the role of silicon on osteoblast function [13, 14, 18]. In particular, a recent study by Reffitt *et al.* [18] demonstrated that silicon stimulated type I collagen synthesis in human osteoblast-like cells and enhanced their differentiation.

The results from this sheep model study combined with the those reported in previous studies [27, 28, 65, 66] provide strong evidence for the role of silicate ions in improving the bioactivity of HA ceramics.

5. Conclusions

Dense granules of phase pure hydroxyapatite, 0.8 and 1.5 wt% silicon-substituted hydroxyapatite, with similar size, morphology, bulk density and packing density were prepared by aqueous precipitation methods. The bioactivity of hydroxyapatite was significantly enhanced with the incorporation of silicate ions into the hydroxyapatite structure. These findings highlight that silicate-substituted hydroxyapatite ceramics are improved alternatives to phase pure hydroxyapatite for biomedical applications.

Acknowledgments

The authors would like to thank the Engineering and Physical Research Council, Cambridge-MIT (CMI) organisation and ApaTech Ltd., for their financial support.

References

1. K. LEWANDROWSKI, J. D. GRESSER, D. L. WISE and D. J. TRANTOLO, *Biomaterials.* **21** (2000) 757.
2. R. R. BETZ, *Orthopaedics*. **25** (2002) S561.
3. R. BUCHOLZ, in "Bone Grafts, Derivatives and Substitutes," edited by M. R. Urist, B. T. O'Conner and R. G. Burwell (Butterworth-Heinemann Ltd., Oxford, 1994) p. 260.
4. R. BUCHOLZ, A. CARLTON and R. HOLMES, *Clin. Orthop. Rel. Res*. **240** (1989) 53.
5. W. REMAGEN and L. PREZMECKY, *Impl. Dentistry*. **4** (1995) 182.
6. L. M. WOLFORD, R. W. WARDROP and J. M. HARTOG, *J. Oral and Maxillof. Surg*. **45** (1987) 1034.
7. M. JARCHO, J. F. KAY, K. I. GUMAER, R. H. DOREMUS and H. P. DROBECK, *J. Bioengng*. **1** (1976) 79.
8. N. IKEDA, K. KAWANABE and T. NAKAMURA, *Biomaterials*. **20** (1999) 1087.
9. H. OONISHI, L. L. HENCH, J. WILSON, F. SUGIHARA, E. TSUJI, S. KUSHITANI and H. IWAKI, *J. Biomed. Mater. Res*. **44** (1999) 31.
10. G. DACULSI, R. Z. LEGEROS and D. MITRE, *Calcif. Tissue Intern*. **45** (1989) 95.
11. R. Z. LEGEROS, O. R. TRAUTZ, J. P. LEGEROS and E. KLEIN, *Bulletin de la Societe Chimique de France*. (1968) 1712.
12. A. S. POSNER, *Bull. Hosp. Joint Dis.* **39** (1978) 126.
13. E. M. CARLISLE, *Science*. **167** (1970) 279.
14. *Idem.*, *ibid*. **178** (1972) 619.
15. *Idem.*, *Fed. Proc.* **33** (1974) 1758.
16. K. SCHWARZ and D. B. MILNE, *Nature*. **239** (1972) 334.
17. E. M. CARLISLE, *Nutr. Rev.* **40** (1982) 193.
18. D. M. REFFITT, N. OGSTON, R. JUGDAOSINGH, H. F. J. CHEUNG, B. A. J. EVANS, R. P. H. THOMPSON, J. J. POWELL and G. N. HAMPSON, *Bone*. **32** (2003) 127.
19. A. J. RUYS, *J. Austr. Ceram. Soc*. **29** (1993) 83.
20. Y. TANIZAWA and T. SUZUKI, *Phosph. Res. Bull*. **4** (1994) 83.
21. K. SUGIYAMA, T. SUZUKI and T. SATOH, *J. Antibact. Antifung. Agents* **23** (1995) 67.
22. K. S. LESHKIVICH and E. A. MONROE, *J. Mater. Sci*. **28** (1993) 9.
23. L. BOYER, J. CARPENA and J. L. LACOUT, *Solid State Ion*. **95** (1997) 121.
24. I. R. GIBSON, S. M. BEST and W. BONFIELD, *J. Biomed. Mater. Res*. **44** (1999) 422.
25. I. R. GIBSON, L. J. JHA, J. D. SANTOS, S. M. BEST and W. BONFIELD, in "Bioceramics", edited by R. Z. LeGeros and J. P. LeGeros (World Scientific Publishing Co. Pte. Ltd., New York, 1998) Vol. 11, p. 105.
26. I. R. GIBSON, S. M. BEST and W. BONFIELD, *J. Amer. Ceram. Soc*. **85** (2002) 2771.
27. I. R. GIBSON, J. HUANG, S. M. BEST and W. BONFIELD, in "Bioceramics," edited by H. Ohgushi, G. W. Hastings, and T. Yoshikawa (World Scientific Publishing Co. Pte. Ltd., Nara, 1999) Vol. 12, p. 191.
28. N. PATEL, S. M. BEST, W. BONFIELD, I. R. GIBSON, K. A. HING, E. DAMIEN and P. A. REVELL, *J. Mater. Sci.: Mater. Med*. **13** (2002) 1199.
29. M. AKAO, H. AOKI and K. KATO, *J. Mater. Sci*. **16** (1981) 809.
30. M. JARCHO, C. H. BOLEN, M. B. THOMAS, J. BOBICK, J. F. KAY and R. H. DOREMUS, *ibid*. **11** (1976) 2027.
31. I. R. GIBSON, S. KE, S. M. BEST and W. BONFIELD, *J. Mater. Sci.: Mater. Med*. **12** (2001) 163.
32. PDF Card No. 9-432, ICDD, Newton Square, Pennsylvania, USA.
33. E. R. WEIBEL and H. E. ELIAS, in "Quantitative Methods in Morphology" (Spinger-Verlag, Berlin, 1967).
34. W. A. MERZ and R. K. SCHENK, *Acta. Anat.* **76** (1970) 1.
35. K. A. HING, S. M. BEST, K. E. TANNER, P. A. REVELL and W. BONFIELD, *Proc. Instit. Mech. Eng*. **212** (Part H) (1998) 437.
36. K. A. HING, PhD Thesis, University of London, UK, 1996.)
37. G. DE WITH, H. J. A. VAN DIJK, N. HATTU and K. PRIJS, *J. Mater. Sci*. **16** (1981) 1592.
38. A. CUNEYT TAS, F. KORKUSUZ, M. TIMUCIN and N. AKKAS, *J. Mater. Sci.: Mater. Med*. **8** (1997) 91.
39. N. PATEL, I. R. GIBSON, S. KE, S. M. BEST and W. BONFIELD, *ibid*. **12** (2001) 181.
40. P. E. WANG and T. K. CHAKI, *ibid*. **4** (1993) 150.
41. R. Z. LEGEROS and J. P. LEGEROS, in "Introduction to Bioceramics," edited by L. L. Hench and J. Wilson (World Scientific Publishing Co., Singapore, 1993) p. 139.
42. T. S. B. NARASARAJU and D. E. PHEBE, *J. Mater. Sci*. **31** (1996) 1.
43. R. Z. LEGEROS, R. KIJKOWSKI, C. BAUTISTA and J. P. LEGEROS, *Connect. Tissue Res*. **33** (1995) 203.
44. R. Z. LEGEROS, M. A. MIRAVITE, G. B. QUIROLGICO and M. E. J. CURZON, *Calcif. Tissue Res*. **S22** (1977) 362.
45. J. G. J. PEELEN, B. V. REJDA and K. DE GROOT, *Ceram. Intern*. **4** (1978) 71.
46. H. W. DENISSEN, K. DE GROOT, A. A. DRIESSEN, J. G. C. WOLKE, J. G. J. PEELEN, H. J. A. VAN DIJK, A. P. GEHRING and P. J. KLOPPER, *Sci. Ceram.* **10** (1980) 63.
47. J. MERRY, PhD Thesis, University of London, UK, 2000.
48. R. D. SHANNON and C. T. PREWITT, *Acta. Cryst.* **B25** (1969).
49. N. PATEL, E. L. FOLLON, I. R. GIBSON, S. M. BEST and W. BONFIELD, *Key Eng. Mat.* **240–242** (2003) 919.
50. D. J. SIMMONS, in "The Biochemistry and Physiology of Bone," edited by G. H. Bourne (Academic Press, New York, 1976) p. 445.

51. D. M. NUNAMAKEN, *Clin. Orthop*. **355** (1998) S65.
52. G. S. STALLER, D. W. RICHARDSON, D. M. NUNAMAKEN and M. PROVOST, *Vet. Surg.* **24** (1995) 299.
53. B. FLAUTRE, C. DELECOURT, M. C. BLARY, P. VAN LANDUYT, J. LEMAITRE and P. HARDOUIN, *Bone*. **25** (1999) 35S.
54. R. Z. LEGEROS, I. ORLY, M. GREGOIRE and G. DACULSI, in "The Bone-Biomaterial Interface," edited by J. E. Davies (University of Toronto press, Toronto, 1991) p. 76.
55. G. DACULSI, R. Z. LEGEROS, M. HEUGHEBAERT and I. BARBIEUX, *Calcif. Tissue Intern.* **46** (1990) 20.
56. P. DUCHEYNE and Q. QIU, *Biomaterials* **20** (1999) 2287.
57. T. KOKUBO, H. M. KIM, M. KAWASHITA and T. NAKAMURA, in "Bone Engineering," edited by J. E. Davies (EM Squared Inc., Toronto, 2000) p. 190.
58. C. LOTY, J. M. SAUTIER, H. BOULEKBACHE, T. KOKUBO, H. M. KIM and N. FOREST, *J. Biomed. Mater. Res*. **49** (2000) 423.
59. K. NISHIO, M. NEO, S. NISHIGUCHI, H. M. KIM, T. KOKUBO and T. NAKAMURA, *ibid*. **52** (2000) 652.
60. C. P. A. T. KLEIN, A. A. DRIESSEN, K. DE GROOT and A. VAN DEN HOOFF, *ibid*. **17** (1983) 769.
61. K. DE GROOT, in "Biocompatibility of Implant Materials," edited by D. F. Williams (CRC Press, Boca Raton, Florida, 1981) Vol. 1, p. 199.
62. C. A. VAN BLITTERSWIJK, H. LEENDERS, J. VAN DEN BRINK, Y. P. BOVELL, J. D. BRUIJN and K. DE GROOT, in Proc. 19th Ann. Meeting of the Society for Biomaterials (Birmingham Al, 1993) p. 337.
63. J. D. DE BRUIJN, Y. P. BOVELL and C. A. VAN BLITTERSWIJK, *Biomaterials* **15** (1994) 543.
64. J. D. LAYANI, F. J. G. CUISINIER, P. STEUER, H. COHEN, J. C. VOEGEL and I. MAYER, *J. Biomed. Mater. Res*. **50** (2000) 199.
65. A. E. PORTER, N. PATEL, J. N. SKEPPER, S. M. BEST and W. BONFIELD, *Biomaterials* **25** (2004) 3303.
66. A. E. PORTER, N. PATEL, J. N. SKEPPER, S. M. BEST and W. BONFIELD, *ibid*. **24** (2003) 4609.

Received 1 July
and accepted 1 November 2004